https://doi.org/10.5194/angeo-2019-119
Preprint. Discussion started: 29 August 2019

Annales Geophysicae Discussions

The increase of curvature radius of geomagnetic field lines preceding a classical dipolarization

Osuke Saka
Office Geophysik, Ogoori, 838-0141, Japan

Abstract

Downstream observations at geosynchronous altitudes of field line dipolarization exhibit fundamental component of substorms associated with high velocity magnetotail flow bursts referred to as Bursty Bulk Flows. In growth phase of substorms, we found that the magnetosphere at geosynchronous orbit are in unstable conditions for Ballooning instability due to the appreciable tailward stretching of the flux tubes, and for slow magnetoacoustic wave due to the continuing field-aligned inflows of plasma sheet plasmas towards the equatorial plane. We propose following scenario of field line dipolarization in downstream locations; (1) The slow wave was excited through Ballooning instability by the arrival of Dipolarization Front at the leading edge of Bursty Bulk Flows. (2) In the equatorial plane, slow wave stretched the flux tube in dawn-dusk directions, which resulted in the spreading plasmas in dawn-dusk directions and reducing the radial pressure gradient in the flux tube. (3) As a result, the flux tube becomes a new equilibrium geometry in which curvature radius of new field lines increased in meridian plane, suggesting an onset of field line dipolarization. (4) Increasing curvature radius induced inductive electric fields of the order of few mV/m pointing westward in the equatorial plane, as well as radial electric fields associated with stretching flux tubes in dawn-dusk directions. Westward electric fields transmitted to the ionosphere produce a dynamic ionosphere where the E layer contains both dynamo ($\mathbf{E}\cdot\mathbf{J}<0$) and dissipation ($\mathbf{E}\cdot\mathbf{J}>0$) processes in it for generating field-aligned current system of Bostrom type. The dipolarization processes associated with changing the curvature radius occurred in the transitional intervals lasting for about 10 minutes preceding classical dipolarization composed of reduction of cross-tail currents and pileup of the magnetic fields transported from the tail.

1. Introduction

Substorms are spatially localized and temporarily variable processes in the nighttime magnetosphere. It is often difficult to determine onset timing of substorm processes such as

https://doi.org/10.5194/angeo-2019-119
Preprint. Discussion started: 29 August 2019

magnetotail flow burst, field line dipolarization, and particle injections. To resolve the timing uncertainties, auroras in global satellite images [Nakamura et al., 2001; Miyashita et al., 2009], intensifications of auroral kilometric radiation [Fairfield et al., 1999; Morioka et al., 2010], and dispersionless particle injection in geosynchronous orbit [Birn et al., 1997] were used. Ground Pi2 pulsations are another useful tool for determination of the substorm timing [Sakurai and Saito, 1976; Nagai et al., 1998; Baumjohann et al., 1999]. Particularly, Pi2s in equatorial region exhibited small phase difference (m<1, m denotes azimuthal wave number) across widely separated stations in the equatorial countries [Kitamura et al., 1998]. This enabled us accurate onset timing study using magnetometer data from two remote locations, geosynchronous altitudes and conjugate ground stations of the equatorial countries [Saka et al., 2010].

In this study, we focus on the dipolarization events at geosynchronous orbit from growth to expansion phase. Triggering mechanisms of the field line dipolarization in the vicinity of geosynchronous orbit are our major concern. In this paper, onset timing study using magnetometer data from equatorial countries [Saka et al., 2010] are summarized in Sect. 2. In Sect. 3, we present a pre-onset scenario leading to the dipolarization onset. We will focus on the field line dipolarization in the vicinity of geosynchronous orbit in Sect. 4. A coupling of magnetosphere and ionosphere associated with this dipolarization scenario will be presented in Sect. 5. Summary and discussion of this scenario is given in Sect. 6.

2. Summary of onset timing study using ground Pi2s at the equator

In this section, we summarize field line dipolarization occurring at the geosynchronous orbit based on the results obtained by Saka et al. [2010]. In this paper, magnetometer data from geosynchronous satellites (Goes5 and Goes6) and those at ground equatorial stations (Huancayo, Peru) in the conjugate meridian were compared. Goes5 was located at higher latitudes, 10.3 degrees N in dipole coordinates, and Goes6 was closer to the equator; 7.9 degrees N in dipole coordinates. This difference was caused by the separated meridians of the satellites (285 degrees for Goes5, 252 degrees for Goes6). The dipole coordinate used are equivalent to the HDV coordinates; H is positive northward along the dipole axis, V is radial outward, and D denotes dipole east. The field line dipolarization at the geosynchronous orbit can be characterized either by a step-like or impulsive increase of inclination angle of the geomagnetic field lines. The inclination angle is measured positive northward from the dipole equator. The step-like dipolarization was observed by Goes5 located at higher latitudes, while the dipolarization pulse was observed by Goes6 at latitudes closer to the equatorial plane.

https://doi.org/10.5194/angeo-2019-119
Preprint. Discussion started: 29 August 2019

Annales Geophysicae Discussions

The onset of field line dipolarization preceded the initial peak of the ground Pi2 pulse by two minutes, suggesting that the onset was initiated in association with the first increase of the Pi2 amplitudes. Following the dipolarization onset on the ground, field line magnitude decreased at the geosynchronous orbit, and field lines deflected westward (eastward) in the dawn (dusk) sector. Field line deflections decreased the field magnitudes therein by the longitudinal expansion of flux tubes. Decrease of field magnitudes and westward deflections of field lines lasted for 10 minutes. Eastward deflections in the dusk sector, however, continued over this characteristic 10-min-interval. After this 10-min-interval, field magnitudes turned to increase by accompanying a collapse of geomagnetic field lines caused by reappearance of energetic particles of outer radiation belt. It is suggested that classical dipolarization, caused by the reduction of cross-tail currents in the midnight magnetosphere, happened after the nightside magnetosphere experienced this characteristic 10-min-interval. For this reason, the first 10 min intervals are referred to as transitional state of substorm expansion.

In the pre-onset intervals, decrease of the field line inclination started two hours prior to the dipolarization onset. It attained minimum angles (33.6 degrees for Goes5 and 49.4 degrees for Goes6 in dipole coordinates) right before the dipolarization onset.

3. Pre-onset intervals leading to field line dipolarization

One of the properties of plasmas at geosynchronous orbit in pre-onset intervals are continuing inflows of plasma sheet plasmas towards the equatorial plane [Saka and Hayashi, 2017]. The plasma sheet ions and electrons showed predominantly perpendicular temperature anisotropies in the pre-onset intervals. The perpendicular anisotropies gradually decreased towards the onset by increasing the parallel flux. At the onset, however, increase of parallel flux stopped and perpendicular anisotropy increased again [Birn et al., 1997]. This transition of the temperature anisotropy may be accounted for by the following manner. A continuing tailward stretch of the field lines in the pre-onset intervals as depicted in Figure 1 may produce parallel component by the relation,

$$\delta F_{//} = F_{\perp}(\omega \cdot \delta t) \qquad (1)$$

Here, $\delta F_{//}$ denotes increase of parallel flux per time δt, ω is angular velocity of counterclockwise rotation of the inflow ($F_{\perp}$) vectors associated with the thinning of the flux tubes caused by stretching.

Continuing parallel flux associated with the flux tube thinning in the pre-onset intervals may increase plasma pressures in the flux tube at its tailward end. This condition leads to further stretching of the flux tube [Ohtani and Tamao, 1993; Rubtsov et al., 2018] by the relation,

https://doi.org/10.5194/angeo-2019-119
Preprint. Discussion started: 29 August 2019

Annales Geophysicae Discussions

$$\frac{\beta}{2}\kappa + \kappa_B + \frac{1}{R} = 0 \qquad (2)$$

Here, β is plasma to magnetic pressure ratio, κ and κ_B denote reciprocal spatial scales of radial inhomogeneity of plasma pressure and magnetic field in the equatorial plane, respectively. R is curvature radius of the field lines. A further increase of κ associated with more steeper pressure gradient in earthward direction caused by a stimulus may trigger Ballooning instability [Rubtsov et al., 2018].

An increase of parallel flux may also lead to the unstable condition for slow magnetoacoustic wave. After manipulating a set of linearized MHD equations [Kadomtsev, 1976], we have a relation between parallel displacement along the field lines (ξ_z) and perpendicular stretching of the field lines ($\xi_\perp$) in the following form,

$$\xi_z = \frac{C_S^2}{\omega^2} F \cdot B_0^2 \frac{\partial}{\partial z}(div\,\xi_\perp) \qquad (3)$$

Here, C_s, ω and B_0 are the sound velocity, angular frequency of waves and background field magnitudes, respectively. *F* is given by

$$F = \frac{C_A^2}{B_0^2} \frac{1}{C_s^2 - (\frac{\omega}{k})^2} \qquad (4)$$

F is positive for the slow magnetoacoustic wave and negative for the fast magnetoacoustic wave. C_A denotes Alfven velocity. If the wave mode was the fast mode, flux tubes would have contracted in longitudes towards the midnight sector, which was not observed during the transitional state of substorm expansion (see Section 2).

It is therefore expected in the pre-onset intervals that slow magnetoacoustic wave coupled with Alfven wave are in unstable conditions. These waves can be excited by the Ballooning instability [Ohtani and Tamao,1989; Rubtsov et al., 2018] if the instability was triggered by a stimulus.

4. Field line dipolarization in the vicinity of geosynchronous orbit

We can assume the westward electric fields in Dipolarization Front (DF) [Runov et a., 2011] embedded in the leading edge of Bursty Bulk Flow (BBF) as external stimulus for triggering Ballooning instability [Saka, 2019]. In this case westward electric fields in the DF temporarily amplified the parallel flux towards the end point of the flux tube in the equatorial plane and steepen earthward pressure gradient. If it exceeds instability threshold determined by β and initial curvature radius *R*, slow magnetoacoustic wave can be excited [Rubtsov et al., 2018]. Once the slow magnetoacoustic wave was excited, stretched flux tubes in the

https://doi.org/10.5194/angeo-2019-119
Preprint. Discussion started: 29 August 2019

equatorial pane as depicted in Figure 2 spread the plasmas in dawn-dusk directions and smooth the radial gradient of plasma pressures in the equatorial plane (smaller κ). Spread of plasmas in dawn-dusk directions were observed as increasing perpendicular anisotropies [Birn et al., 1997] or increasing perpendicular fluxes [Saka and Hayashi, 2017] at geosynchronous orbit. This may result in the transition of the flux tube geometry to a new configuration, an increase of the curvature radius of the field lines (larger *R*) (see equation (2)).

On the other hand, field lines in the further earthward locations may be compressed by the inward movement of the outer field lines. This process associated with the dipolarization onset may increase the parameter κ_B in equation (2) which may result in transition to a new geometry of earthward field lines, a decrease of the curvature radius *R*. Transition of the field line geometries for onset locations and ones in earthward locations are schematically illustrated in Figure 3. These field line geometries matched the third harmonic and fundamental harmonic deformations of outer and inner field lines, respectively, associated with Pi2 onset [Saka et al., 2012]. Transitions of the flux tube geometry in magnetosphere also correspond to the production of negative bay in higher latitudes and positive bay in lower latitudes. If we can assume that negative bay switched to positive bay at latitudes, 60 degrees in geomagnetic coordinates for examples, this latitude can be mapped beyond the geosynchronous orbit (L~7 Re or further tailward) as field line dipolarization occurs along the stretched flux tubes. Consequently, this scenario requires that the BBFs are not necessary to reach inner magnetosphere to trigger the substorm onset at lower latitudes.

Increasing of the curvature radius, or shrinkage of the flux tubes in meridian plane, produce a reduction of the radial component of the field lines (V in dipole coordinates) by adding positive V in the north of the equatorial plane and negative V in the south. If amplitudes of the V component changed by 10 nT in one minute, the expected inductive electric fields (westward) could be of the order of 1.0 mV/m when these electric field were confined within 1 Re from the equatorial plane. The dawn-dusk expansion of the flux tubes may also produce inductive electric fields (earthward and tailward in dawn and dusk sector, respectively) of the same order of magnitudes. The westward electric fields produce earthward flow bursts referred to as convection surge. The inductive electric fields produced by the dipolarization are the same order of magnitudes observed in DF [Runov et al., 2011]

5. Coupling of magnetosphere and ionosphere in association with field line dipolarization

The inductive electric fields may be transmitted along the field lines as poloidally and

https://doi.org/10.5194/angeo-2019-119
Preprint. Discussion started: 29 August 2019

Annales Geophysicae Discussions Open Access EGU

toroidally polarized Alfven waves [Klimushkin et al., 2004]. These electric fields produce a dynamic ionosphere in polar region that includes nonlinear evolution of ionospheric plasmas (poleward expansion), as well as production of field-aligned currents and parallel potentials by exciting ion acoustic wave in quasi-neutral condition [Saka, 2019]. It is not the aim of this paper to describe in detail the dynamic processes in the ionosphere, but to show a local production of currents in the ionosphere as well as field-aligned currents by the penetrated electric fields. For this purpose, we revisit the 10 August 1994 substorm event studied by Saka and Hayashi [2017]. In this event, eastward expansion was observed of the field line dipolarization region. At the leading edge of the expansion, ground magnetometer data showed bipolar event (quick change of the D component from positive to negative in about 5 min), being confined in the expanding dipolarization front as a substructure. The substructure in the leading edge of the field line dipolarization will be examined as follows.

We can assume that magnetic signals on the ground are associated with the sum of the horizontal Hall currents in the ionosphere [Fukushima, 1971]. These currents can be calculated by the relation,

$$(rot\,\mathbf{J})_Z = -\frac{1}{\mu_0}\nabla^2 B_Z \qquad (5)$$

We used the ground vertical component (b) as a proxy of B_z in the ionosphere. The second derivative in right-hand side of equation (5) is approximated as,

$$\nabla^2 B_Z^i = \left(\frac{b^{i+1}-b^i}{L_{i+1}-L_i}-\frac{b^i-b^{i-1}}{L_i-L_{i-1}}\right)/\left(L_{i+1}-L_{i-1}\right) \qquad (6)$$

Here, i denotes i-th station in the meridian chain. L_i is the geomagnetic latitude of the i-th station. We considered meridional change only. This is because the vertical component changed from negative to positive across the meridian, while in longitudes it changed simply decreasing or increasing in lower and higher latitudes after onset, respectively. The results reproduced from Saka and Hayashi [2017] are shown in Figure 4(A). The dipolarization front crossed this meridian at 12:13 UT corresponding to the interval labelled 1. Two points arose from this figure; (1) Hall current pair existed, CCW in the lower latitudes and CW in the higher latitudes, (2) These current patterns expand poleward. Current patterns in the interval from 1 to 5 in Figure 4(A) are illustrated in Figure 4(B) to facilitate the poleward expansion. It is clearly demonstrated that current pair forming CW in higher latitudes and CCW in lower latitudes expanded in time towards the pole. Bipolar change can be recorded in the D component data (not shown) when the ground station, FSIM in this case, passes from segment 1 to 2 in Figure 4(B). As a result, dipolarization front expanded eastward progressively by producing the poleward expansion at each meridian. The front left behind the current pattern comprising upward field-aligned currents in lower latitudes and downward

https://doi.org/10.5194/angeo-2019-119
Preprint. Discussion started: 29 August 2019

in higher latitudes, or Bostrom type current system. We propose that the ionosphere itself has inherent dynamo in the E layer to drive this Bostrom type current system. The reasons are as follows;

In the E region, drift trajectories may be written [Kelley, 1989] for electrons by,

$$\mathbf{U}_{e\perp} = \frac{1}{B}[\mathbf{E} \times \hat{\mathbf{B}}] \qquad (7)$$

and for ions by,

$$\mathbf{U}_{i\perp} = b_i[\mathbf{E} + \kappa_i \mathbf{E} \times \hat{\mathbf{B}}]. \qquad (8)$$

Here, b_i is mobility of ions defined as $\Omega_i/(B\nu_{in})$, κ_i is defined as Ω_i/ν_{in}. Symbols Ω_i and ν_{in} are ion gyrofrequency and ion-neutral collision frequency, respectively. $\hat{\mathbf{B}}$ denotes a unit vector of the magnetic fields B. We assumed that $\mathbf{E} \times \mathbf{B}$ drifts for electrons and ions were driven by westward electric fields transmitted from the magnetosphere. Because of very low mobility of ions in E layer ($\kappa_i = 0.1$), electric field drifts accumulate electrons (not ions) in lower latitudes and produce secondary southward electric fields in the ionosphere. The southward electric fields produced southward motion of ions due to the first term of equation (8). They carry Pedersen currents (ion currents) for producing quasi-neutrality of ionosphere. $\mathbf{E}_W \times \mathbf{B}$ drifts caused by the transmitted westward electric fields ($\mathbf{E}_W$) may propel electrons against southward electric fields from higher latitudes to lower latitudes ($\mathbf{E}_S \cdot \mathbf{J} < 0$, dynamo) to maintain the potential drop for driving Pedersen currents ($\mathbf{E}_S \cdot \mathbf{J} > 0$, dissipation). This means the ionospheric E layer contains both dynamo (E layer dynamo) and dissipation processes in it. In quasi-neutral condition, a small imbalance of particle densities of electrons and ions ($\delta n :\ 10^2 m^{-3}$) may induce in lower latitudes negative potential region of the order of -100 kV with horizontal scale length of 100 km. To sustain this negative potential, upward field-aligned currents of the order of $1.0 \mu A/m^2$ for $\Sigma_P \sim 10^0 S$ must flow. Downward field-aligned currents from the positive potential regions in the higher latitudes may also be expected. It is supposed that upward field-aligned currents may be composed of ions and downward currents are electrons to require stable equatorward ion flows in the Pedersen channel. Those field-aligned currents closing via Pedersen currents in the ionosphere and polarization currents in the magnetosphere comprised meridional current system of Bostrom type, or incomplete Cowling channel [Baumjohann, 1983]. They were driven by the E layer dynamo.

https://doi.org/10.5194/angeo-2019-119
Preprint. Discussion started: 29 August 2019

6. Discussion and Summary

Definition of field line dipolarization is a configuration change from stretching to shrinkage of geomagnetic field lines in the midnight meridian of magnetosphere. Two models have been proposed to account for the configuration change; diversion of the cross-tail currents via ionosphere, referred to as substorm current wedge (SCW), as first proposed in McPherron et al. [1973] and extinction of the cross-tail currents by a local kinetic instability, current disruption (CD) [Lui, 1996]. These models have been adopted for many decades to account for the critical issues associated with substorm onset. We propose, based on Ballooning instability scenario, that field line dipolarization is caused by the slow magnetoacoustic wave in which a small curvature radius of the stretched field lines in pre-onset intervals increased by spreading plasmas in the equatorial plane towards dawn-dusk directions. Dipolarization regions expand in longitudes toward dayside sector and decrease field magnitudes by expanding flux tubes therein. This condition continued for about 10 min and subsided when the nightside magnetosphere collapsed by the refilling of the energetic particles from the outer radiation belt. After that, classical dipolarization caused by the reduction of cross-tail currents or pileup of the magnetic flux transported from the tail begins. For this reason, the first 10 min intervals of Pi2 onset are referred to as transitional state of the substorm expansion [Saka et al., 2010]. We emphasize that two different types of the dipolarization exist in the substorms; one is associated with change of curvature radius of field lines in the transitional state and the other is subsequent pileup of the magnetic flux transported from the tail. Tailward regression of the dipolarization region as reported in Baumjohann et al. [1999] may be associated with the latter case.

In the transitional state lasting for about 10 min, the inductive electric fields pointing westward were produced in the equatorial plane. They propagated along the field lines to the ionosphere to produce dynamic ionosphere in the polar regions. The dynamic ionosphere has inherent dynamo processes in E layer producing meridional field-aligned currents of the Bostrom type (downward in higher latitudes and upward in lower latitudes). We found that Bostrom type current system was indeed observed on the ground at the front of dipolarization expanding towards east. The magnetospheric dynamo produced by earthward electric fields in the equatorial plane [Akasofu, 2003] and the E layer dynamo in the ionosphere worked together to activate the Bostrom current system.

7. Code/Data availability

No data sets were used in this article.

8. Competing interest

https://doi.org/10.5194/angeo-2019-119
Preprint. Discussion started: 29 August 2019

The author declares that there is no conflict of interest.

Acknowledgements

The author would like to express his sincere thanks to all the members of Global Aurora Dynamics Campaign (GADC) [Oguti et al., 1988].

References

Akasofu, S.-I.: Source of auroral electrons and the magnetospheric substorm current system, J. Geophys. Res., 108, A4, 8006, doi:10.1029/2002JA009547, 2003.

Baumjohann, W.: Ionospheric and field-aligned current systems in the auroral zone: A concise review, Adv. Space Res., 2, 55-62, 1983.

Baumjohann, W., Hesse, M., Kokubun, S., Mukai, T., Nagai, T., and Petrukovich, A.A.: Substorm dipolarization and recovery, J. Geophys. Res., 104, 24995-25000, 1999.

Birn, J., Thomsen, M.F., Borovsky, J.E., Reeves, G.D., McComas, D.J., and Belian, R.D.: Characteristic plasma properties during dispersionless substorm injections at geosynchronous orbit, J. Geophys. Res., 102, A2, 2309-2324, 1997.

Fairfield, D.H., Mukai, T., Brittnacher, M., Reeves, G.D., Kokubun, S., Parks, G.K., Nagai, T., Mtsumoto, H., Hashimoto, K., Gurnett, D.A., and Yamamoto, T.: Earthward flow bursts in the inner magnetotail and their relation to auroral brightenings, AKR intensifications, geosynchronous particle injections and magnetic activity, J. Geophys. Res., 104, A1, 355-370, 1999.

Fukushima, N.: Electric current systems for polar substorms and their magnetic effect below and above the ionosphere, Radio Sciences, 6, 269-275, 1971.

Kadomtsev, B.B.: Collective phenomena in plasmas (in Japanese), Iwanami shoten, Tokyo, 1976.

Kelley, M.C.: The earth's ionosphere: plasma physics and electrodynamics, Academic Press, Inc, 1989.

Kitamura, T., Saka, O., Shimoizumu, M., Tachihara, H., Oguti, T., Araki, T., Sato, N., Ishitsuka, M., Veliz, O., and Nyobe, J.B.: Global mode of Pi2 waves in the equatorial region: Difference of Pi2 mode between high and equatorial latitudes, J. Goomag. Geoelectr, 40, 621-634, 1988.

Klimushkin, D.Yu., Mager, P.N., and Glassmeier, K.-H.: Toroidal and Poloidal Alfven waves with arbitrary azimuthal wave numbers in a finite pressure plasma in the Earth's magnetosphere, Annales Geophysicae, 22, 267-287, 2004.

https://doi.org/10.5194/angeo-2019-119
Preprint. Discussion started: 29 August 2019

Annales Geophysicae Discussions

Lui, A.T.Y.: Current disruption in the Earth's magnetosphere: Observations and models, J. Geophys. Res., 101, 13067-13088, 1996.

McPherron, R.L., Russell, C.T., and Aubry, M.P.: Satellite studies of magnetospheric substorms on August 15, 1968: 9. Phenomenological model for substorms, J. Geophys. Res., 78, 3131-3148, 1973.

Miyashita, Y., Machida, S., Kamide, Y., Nagata, D., Liou, K., Fujimoto, M., Ieda, A., Saito, M.H., Russell, C.T., Christon, S.P., Nose, M., Frey, H.U., Shinohara, I., Muaki, T., Saito, Y., and Hayakawa, H.: A state-of-the-art picture of substorm-associated evolution of the near-Earth magnetotail obtained from superposed epoch analysis, J. Geophys. Res., 114, A01211, doi:10.1029/2008JA013225, 2009.

Morioka, A., Miyoshi, Y., Miyashita, Kasaba, Y., Misawa, H., Tsuchiya, F., Kataoka, R., Kadokura, A., Mukai, T., Yumoto, K., Menietti, D.J., Parks, G., Liou, K., Honary, and Donovan, E.: Two-step evolution of auroral acceleration at substorm onset, J. Geophys. Res., 115, A11213, doi:10.1029/2010JA015361, 2010.

Nagai, T., Fujimoto, M., Saito, Y., Machida, S., Terasawa, T., Nakamura, R., Yamamoto, T., Mukai, T., Nishida, A., and Kokubun, S.: Structure and dynamics of magnetic reconnection for substorm onsets with Geotail observations, J. Geophys. Res., 103, A3, 4419-4440, 1998.

Nakamura, R., Baumjohann, W., Brittnacher, M., Sergeev, V.A., Kubyshkina, Mukai, T., and Liou, K.: Flow bursts and auroral activations: Onset timing and foot point location, J. Geophys. Res., 106, A6, 10777-10789, 2001.

Oguti, T., Kitamura, T., and Watanabe, T.: Global aurora dynamics campaign, 1985-1986, J. Geomag. Geoelectr, 40, 485-504, 1988.

Ohtani, S.-I., Miura, A., and Tamao, T.: Coupling between Alfven and slow magnetosonic waves in an inhomogeneous finite-β plasma: 1 Coupled equations and physical mechanism, Planet. Space Sci., 37, 567-577, 1989.

Ohtani, S.-I., and Tamao, T.: Does the ballooning instability trigger substorms in the near-earth magnetotail?, J. Geophys. Res., 98, A11, 19369-19379, 1993.

Rubtsov, A.V., Mager, P.N., and Klimushkin, D.Yu.: Ballooning instability of azimuthally small scale coupled Alfven and slow magnetoacoustic modes in two-dimensionally inhomogeneous magnetospheric plasma, Physics of Plasmas 25, 102903, doi:10.1063/1.5051474, 2018.

Runov, A., Angelopoulos, V., Zhou, X.-Z., Zhang, X.-J., Li, S., Plaschke, F., and Bonnell, J.: A THEMIS multicase study of dipolarization fronts in the magnetotail plasma sheet, 116, A05216, doi:10.1029/2010JA016316, 2011.

Saka, O. Hayashi, K, and Thomsen, M.: First 10 min intervals of Pi2 onset at geosynchronous altitudes during the expansion of energetic ion regions in the nighttime sector, J. Atmos. Solar Terr. Phys., 72, 1100-1109, 2010.

Saka, O., Hayashi, K., and Koga, D.: Excitation of the third harmonic mode in meridian planes for Pi2 in the auroral zone, J. Geophys. Res., 117, A12215, doi:10.1029/2012JA018003, 2012.

Saka, O., and Hayashi, K.: Longitudinal expansion of field line dipolarization, J. Atmos. Solar Terr. Phys., 164, 235-242, 2017.

Saka, O.: A new scenario applying traffic flow analogy to poleward expansion of auroras, Ann. Geophys., 37, 381-387, 2019.

Sakurai, T., and Saito, T.: Magnetic pulsation Pi2 and substorm onset, Planet. Space Sci., 24, 573-575, 1972.

https://doi.org/10.5194/angeo-2019-119
Preprint. Discussion started: 29 August 2019

Annales Geophysicae Discussions Open Access EGU

Figure captions

Figure 1.
A progress of field line thinning in the growth phase is illustrated. The inflow flux ($F_\perp$) rotated counterclockwise, from red, green, and to blue arrows in time. The rotation of the inflow vectors produced the field-aligned component of the flux, $\delta F_{//} = F_\perp(\omega \cdot \delta t)$ as depicted in the inset. Note that inflows are localized earthward of the outer field lines.

Figure 2.
Schematic illustration of the flux tube deformations associated with the slow magnetoacoustic wave. Parallel displacement, ξ_z , along the field lines and perpendicular displacement, $\xi_\perp$, in longitude away from the center are coupled in the slow magnetoacoustic wave (see text for the explanation of equations (3) and (4)).

Figure 3.
A schematic illustration of the field line deformations in the meridian plane associated with the changing curvature radius of the field lines. The outer field lines marked by (1) changed to field lines (2) by increasing its curvature radius to R1 (red-dashed circle) in association with the onset of slow magnetoacoustic wave, while the inner field lines marked by (3) moved to field lines (4) of smaller curvature radius R2 (blue-dashed circle). This transition, (3) to (4), may be caused by the radial gradient of magnetic pressures becoming steeper in association with the inward compression of the field lines (see text).

Figure 4.
(A) Vertical component of $(rot\ \mathbf{J})_Z$ in the meridian chain along 300°E for the interval from 1000 UT to 1500 UT, reproduced from Saka and Hayashi [2017]. Dipolarization onset was at 12:13 UT at this meridian. For the calculation of $(rot\ \mathbf{J})_Z$, vertical component data from RES (83.0°N), CBB (76.6°N), CONT (72.6°N), YKC (68.9°N), FSIM (67.2°N), FSJ (61.9°N), and VIC (54.1 °N) were used (see text). Positive for the clockwise rotation (CW) of ionospheric currents and negative for the counterclockwise rotation (CCW) viewed from above the ionosphere. Amplitudes are color-coded. The scale is shown on the right. Demarcation lines separating CCW and CW in latitudes are marked by dashed line. The demarcation line moved to poleward after the onset. Note that negative $(rot\ \mathbf{J})_Z$ in poleward edge indicates smooth decrease of the Z amplitudes.

https://doi.org/10.5194/angeo-2019-119
Preprint. Discussion started: 29 August 2019

(B) Time progresses of the CW/CCW patterns are illustrated separately in five segments from 1 to 5 marked in Figure 4 (A). The figure demonstrates a progress of CW/CCW pair in time, CW in the poleward and CCW in the equatorward. This pair developed its size after onset showing poleward expansion. The meridional current associated with this current pair, if closed in the equatorial plane via the field-aligned currents, comprised the Bostrom type current system.

https://doi.org/10.5194/angeo-2019-119
Preprint. Discussion started: 29 August 2019

Annales Geophysicae
Discussions

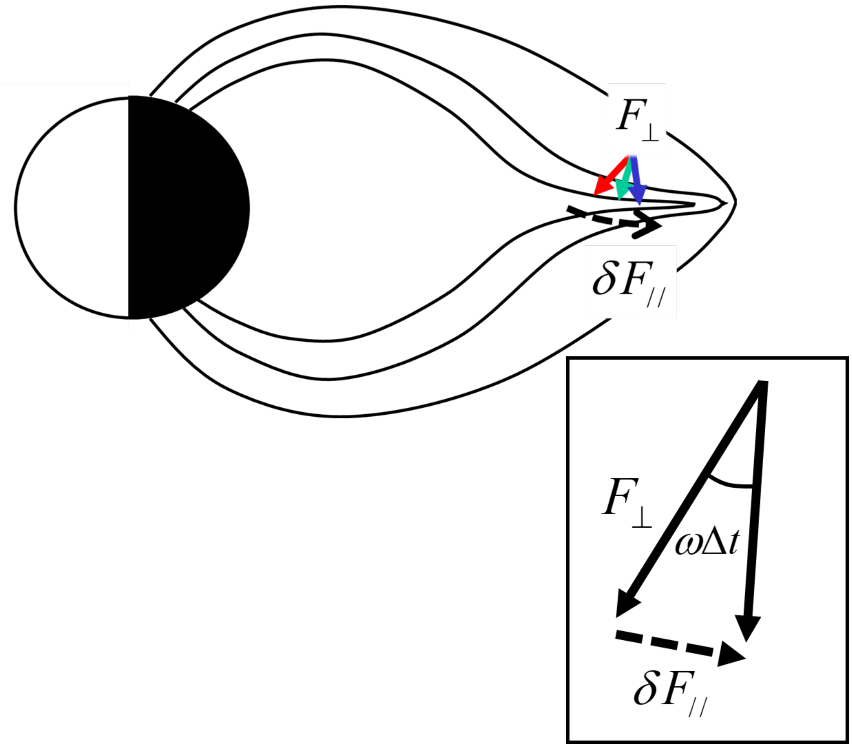

Figure 1

https://doi.org/10.5194/angeo-2019-119
Preprint. Discussion started: 29 August 2019

Annales Geophysicae Discussions
Open Access

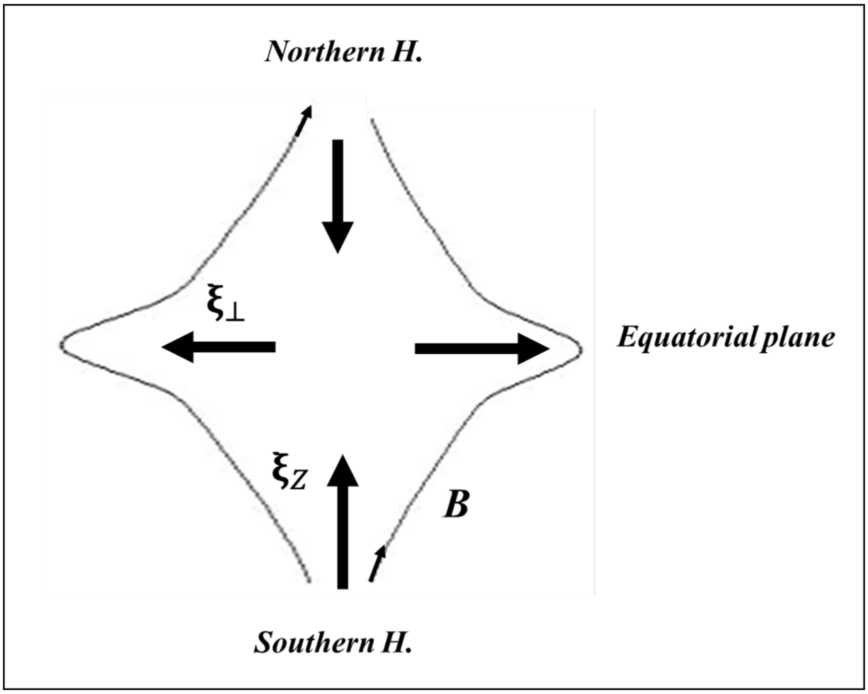

Figure 2

https://doi.org/10.5194/angeo-2019-119
Preprint. Discussion started: 29 August 2019

Annales Geophysicae
Discussions

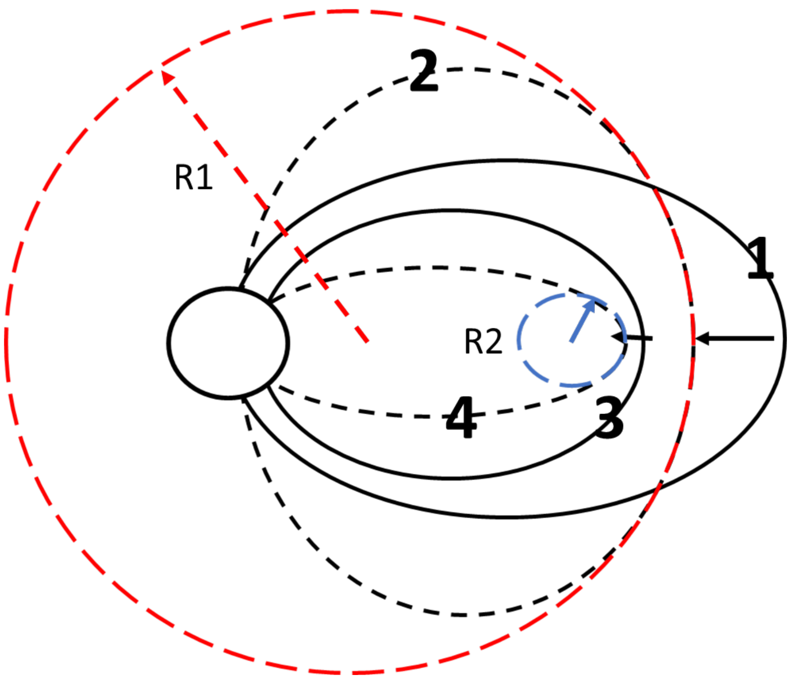

Figure 3

https://doi.org/10.5194/angeo-2019-119
Preprint. Discussion started: 29 August 2019

Annales Geophysicae
Discussions
Open Access
EGU

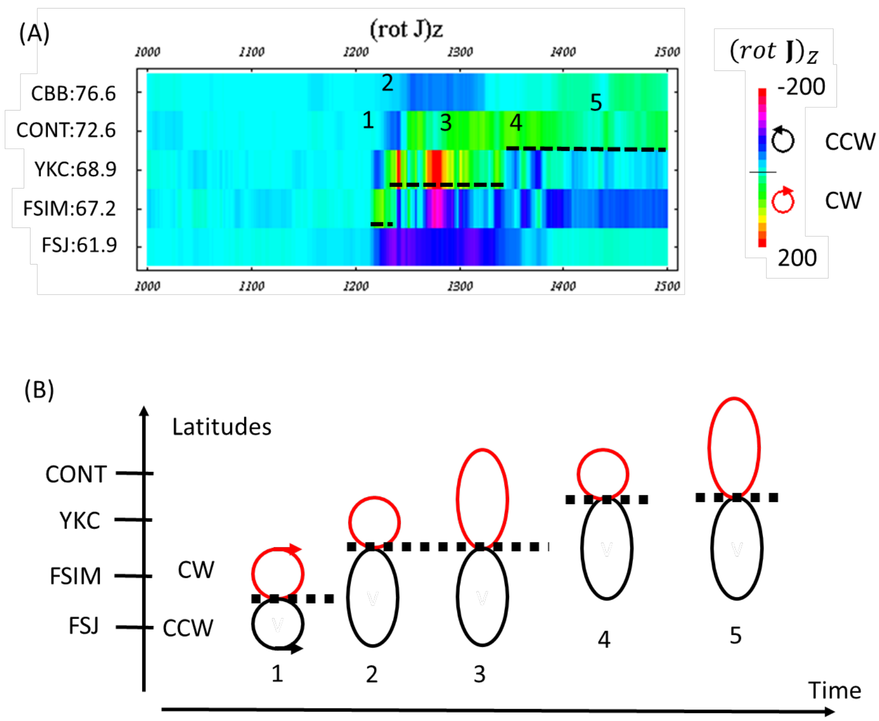

Figure 4